NANO LETTERS

2008
Vol. 8, No. 3
842-847

Carbon Nanotubes as Reinforcement Elements of Composite Nanotools

D. Nakabayashi,[†,‡] A. L. D. Moreau,[‡] V. R. Coluci,[‡] D. S. Galvão,[‡] M. A. Cotta,[‡] and D. Ugarte*[,†,‡]

Laboratório Nacional de Luz Síncrotron, C.P. 6192, 13084-971 Campinas SP, Brazil, and Instituto de Física "Gleb Wataghin", Universidade Estadual de Campinas, UNICAMP, C.P. 6165, 13083-970 Campinas SP, Brazil

Received November 13, 2007; Revised Manuscript Received January 25, 2008

ABSTRACT

Nanotechnology is stimulating the development of nanomanipulators, including tips to interact with individual nanosystems. Fabricating nanotips fulfilling the requirements of shape (size, aspect ratio), mechanical, magnetic, and electrical properties is a material science challenge. Here, we report the generation of reinforced carbon−carbon composite nanotools using a nanotube (CNTs) covered by an amorphous carbon matrix (shell); the CNT tip protruded and remained uncoated to preserve apex size. Unsuitable properties such as flexibility and vibration could be controlled without deteriorating the CNT size, strength, and resilience. Nanomanipulation experiments and molecular dynamics simulations have been used to study the mechanical response of these composite beams under bending efforts. AFM probes based on these C−C composite high aspect ratio tips generated excellent image resolution and showed no degradation after acquiring several hundred (400) images.

The growth of nanoscience and nanotechnology has stimulated the improvement of high spatial resolution techniques that are used to study individual nanosystems. Many projects have built instruments including tips to interact mechanically and electrically with specific regions of nanodevices while observing the process carried out inside scanning electron microscopes.[1–4] Also, the development of equipment including four-probe tips has been reported by different groups, and in some cases each tip can be operated as a scanning tunneling microscope (STM).[5–8] As for manipulation, sharp tips of STM and atomic force microscopy (AFM) have already been used to push and move nanoparticles,[9] carbon nanotubes,[10] nanowires,[11] etc., on flat surfaces. Nanomanipulation procedures require conducting and mechanically strong high aspect ratio nanometric probes; in these terms, the needle-like shape (length $\sim\mu$m, diameter 1–20 nm) of carbon nanotubes (CNTs[12]) renders them an ideal candidate for preparing sharp nanoprobes. Recently, carbon nanotubes have been covered with different metals in order to improve conductivity;[13] these tips were used to create a four-point electrical nanocircuit testing station.[14]

It must be emphasized that few materials show mechanical characteristics (tensile strength in the GPa range) to support bending efforts associated with typical surface forces of the order of nN when shaped into a high aspect ratio beam of nanometric diameter.[15] From this point of view, CNTs seem also to be the best available solution and, in addition, they can be bent easily without breaking, thus allowing a unique and surprising resilience property. But it must be noted that in spite of showing the highest possible tensile strength (40 GPa) and a huge elastic modulus (0.2–1 TPa),[16] their high aspect ratio renders them very flexible; even vibration modes are excited at room temperature,[17] hindering their use in high resolution applications (see example in Figure 1a,b).

Fabrication of nanoprobes fulfilling the requirements of tip size, morphology, and mechanical properties (stiffness, tensile strength, etc.) is in fact quite challenging; the limited understanding of surface interactions and nanomechanical properties represent a great obstacle for development of some aspects of nanotechnology (see detailed discussions in the US National Nanotechnology Initiative Reports dedicated to Instrumentation Development[18]). From another point of view, we must consider that modern technology has been able to produce macroscopic materials with an ensemble of functions by combining several constituents in composites;[19] this aspect should also be extended to nanomaterials and tools. In thinking about shape issues, macroscopic high aspect ratio composite structures (beams) are current and reinforced concrete naturally arises as the typical example; in a few words, steel reinforcement bars support tension and concrete supports compression.

In this work, we have extrapolated the reinforced concrete idea to generate high aspect ratio nanotools by forming a

* To whom correspondence should be addressed. E-mail: ugarte@lnls.br.
† Laboratório Nacional de Luz Síncrotron.
‡ Instituto de Física "Gleb Wataghin", Universidade Estadual de Campinas, UNICAMP.

10.1021/nl0729633 CCC: $40.75
Published on Web 02/23/2008

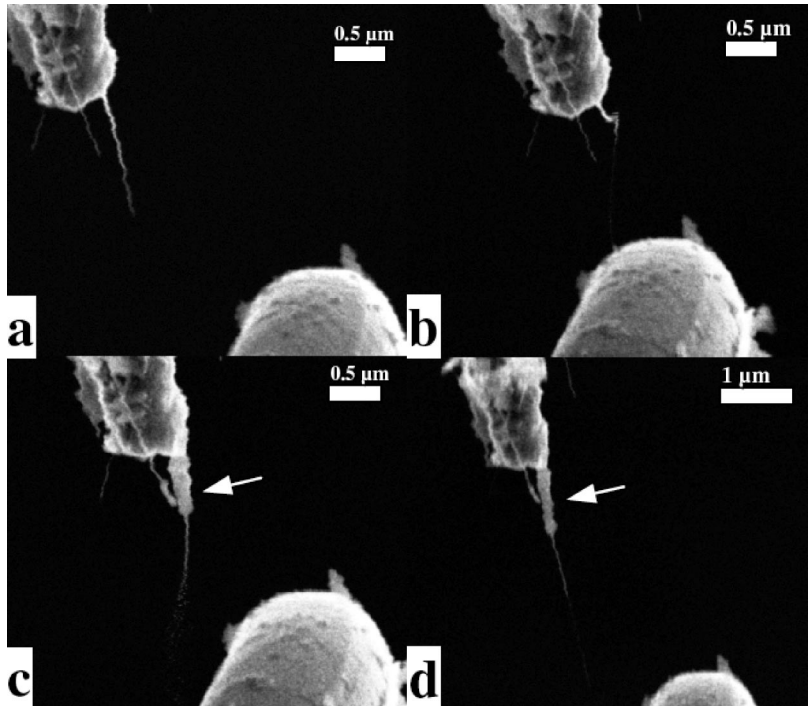

Figure 1. Scanning electron microscope image of a CNT bundle deposited on tungsten tip; the manipulator tip (W) can be seen at the image lower part. (a) CNT deposed on a W tip as prepared; note that the protruding length seems to be ~1.3 μm. (b) When the CNTs touch the opposite manipulator tip, a long CNT stops vibrating and becomes visible; note that carbon nanotubes easily deform when mechanical efforts are applied. (c) After deposition of an a-C shell (thickness 50 nm, length 0.6 μm), the tube becomes visible but still shows thermally activated vibrations. (d) By depositing a ~1 μm long a-C contamination shell, vibrations can be reduced to a negligible level while keeping a very high aspect ratio.

C−C composite using CNT immersed in a diamond-like carbon hard matrix. The mechanical response was tested experimentally using a nanomanipulator in situ in a scanning electron microscope and also analyzed using molecular dynamics simulations. Finally, we have applied this concept to fabricate high resolution and high resistance AFM tips.

Manipulation of CNTs was performed using an in-house built nanomanipulator operating inside a scanning electron microscope equipped with field emission gun (JSM-6330F);[11] electrochemically etched W wires and Si AFM tips were used as support probes. We have used multiwalled carbon nanotubes generated by the electric arc method (20 V, 80 A) method in He atmosphere (500 mbar). Using the manipulator, CNTs were deposited on support tips, where they adhered by van der Waals forces. Then the contact region and subsequently the CNT itself were covered with an a-C layer generated by spontaneous carbon contamination produced by focusing the electron beam on a desired sample position (EBD, electron beam deposited carbon[1,20–23]). The carbon source was the residual hydrocarbon partial pressure in the SEM chamber; the EBD layer deposition has been performed at 25 or 30 kV and ~0.1 nA current. The layer was generated by scanning the beam over the selected region at the highest possible magnification (500000×) while observing the sample in reduced scan area; deposition time was ~20–30 min. The SEM specimen chamber pressure was kept at $\sim 10^{-7}$ Torr using a liquid nitrogen trap; the sample was kept grounded and no charging effects were observed. The nanotubes were kept approximately perpendicular to the beam during deposition and in a unique position; this may raise question about the uniformity of the covering layer thickness. It is generally accepted that the main source of carbon is adsorbed molecules on the object surface, which are cracked by secondary (SE) and back-scattered (BSE) electrons ejected from the sample.[23] A very thin sample, such as a NT, allows the primary SEM beam to traverse it with minor absorption and, in this configuration, SE and BSE are generated all over the NT surface, thus creating a coverage layer all around the nano-object. We must consider that, in addition, the beam was not kept at a fixed position but rather scanning a small area, which can also help to generate a more homogeneous layer. Although we have not analyzed in detail the a-C layer thickness variation around the tubes, we have not observed significant deviations of mechanical behavior when deforming the tubes in different directions. The layer uniformity will certainly be improved by rotating the tube around its axis or at least by depositing the film for a few NT angular positions (for example, SEM specimen holders easily allow a tilt of 30–40°).

Figure 1a shows a CNT bundle with an apparently ~1.3 μm long section hanging beyond an AFM tip; the lower part of the SEM image shows the second tip (W) of the manipulator. By approaching this second tip, we can make a mechanical contact with the protruding CNT; we can then realize that the hanging bundle is actually much longer (~3.3 μm). The thinner region at the bundle extremity remained invisible in the first image; we attribute this fact to the existence of thermally excited vibrations that are stopped when touching the lower tip. If the lower tip is retracted, the long and thin hanging part becomes invisible again. It

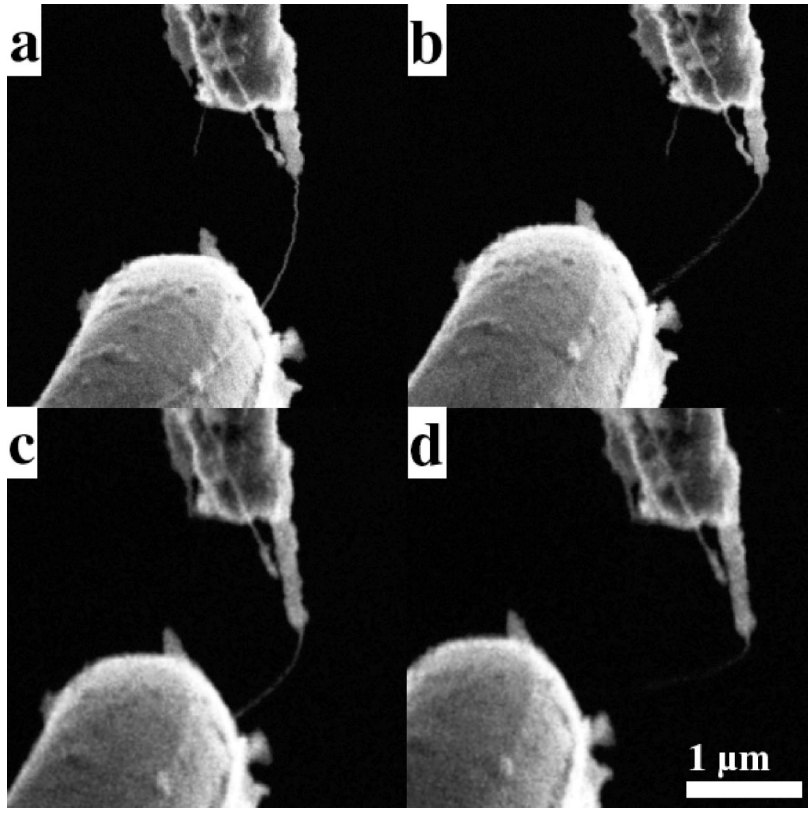

Figure 2. Mechanical deformation of the high aspect ratio composite CNT tip; the composite section is significantly reinforced and lateral efforts generate only deformation on the free CNT region. (a,b) Slight and strong bending of the composite tip when a-C contamination covers the first ~0.6 μm of the hanging CNT. (c,d) Progressive deformation when a longer (~1 μm) a-C shell is deposited on the CNT. Note that, in both cases, the C−C composite section is not deformed and the induced curvature is only produced on the protruding free CNT sector. Severe bending generates an elbow at the region just below the composite region (b,d), revealing a significant reinforcement.

must also be noted that the rather long thin tube is very flexible and it can be easily bent (Figure 1b).

The examples discussed above (Figure 1a,b) reveal some of the major difficulties of using CNT probe tips (vibration and flexibility). Nevertheless, both unsuitable characteristics can be reduced by shortening the hanging section of the tube, which may also generate significant reduction of the aspect ratio. To reduce the undesired effects and keep the needle shape, we have deposited a thin (50 nm) amorphous carbon (a-C) shell generated spontaneously by EBD not only on the contact between tube and AFM tip but along the CNT, creating a coaxial 0.6 μm long a-C shell (see Figure 1c). This shell has not eliminated completely the vibrations, but it can significantly reduce their effect; note that in this situation, the long protruding CNT (still vibrating) becomes clearly visible along its whole length. Vibration can be further reduced to a negligible level by depositing a longer carbon shell (~1 μm in length) along the CNT (Figure 1d). The a-C shell thickness and length can be easily controlled, generating a carbon−carbon nanocomposite close to the bundle attachment region. It must be emphasized that the CNT apex size has been preserved because the tip region remained uncoated; in addition, the deposition of thin a-C layer at the tube base generates a strengthened region without changing significantly the overall aspect ratio.

Further analysis requires that the resistance of this kind of composite nanotube tip be evaluated; Figure 2 displays several snapshots of the application of a progressive deformation of the composite CNT tip by applying a lateral effort using the opposite manipulator tip. Lateral forces induce bending only in the free CNT region and can even form an elbow at the extremity of the nanocomposite region (Figure 2a−d). This emphasizes the enhanced strength of the composite CNT-(a-C) tip sector. Releasing the CNT tip, the tube recovers a straight shape, indicating that the resilience property has been maintained.

We must note that a-C needles generated by EBD of similar size and in identical experimental conditions are extremely fragile, breaking easily at minimal mechanical contact, if not reinforced internally by a CNT (Supporting Information, Figure S1). But as in any fiber reinforced composite material, strength of the interface between the fibers and the matrix is a key issue for the final performance.[19] We speculate that as the a-C shell is deposited by cracking vacuum residual gazes (probably heavy hydrocarbons) with 30 keV energy electrons, the irradiation may also induce the formation of bonds between the shell and the nanotube surface; in fact, strong clamping of CNT on surfaces using EBD carbon layers has already been reported.[1,22,23] This should account for the efficient strengthening of the composite region that does not deform under lateral forces; unfortunately, our experimental nanomanipulation setup do not allow the quantitative measurement of applied forces.[24–26] Then, to gather further insight into atomistic

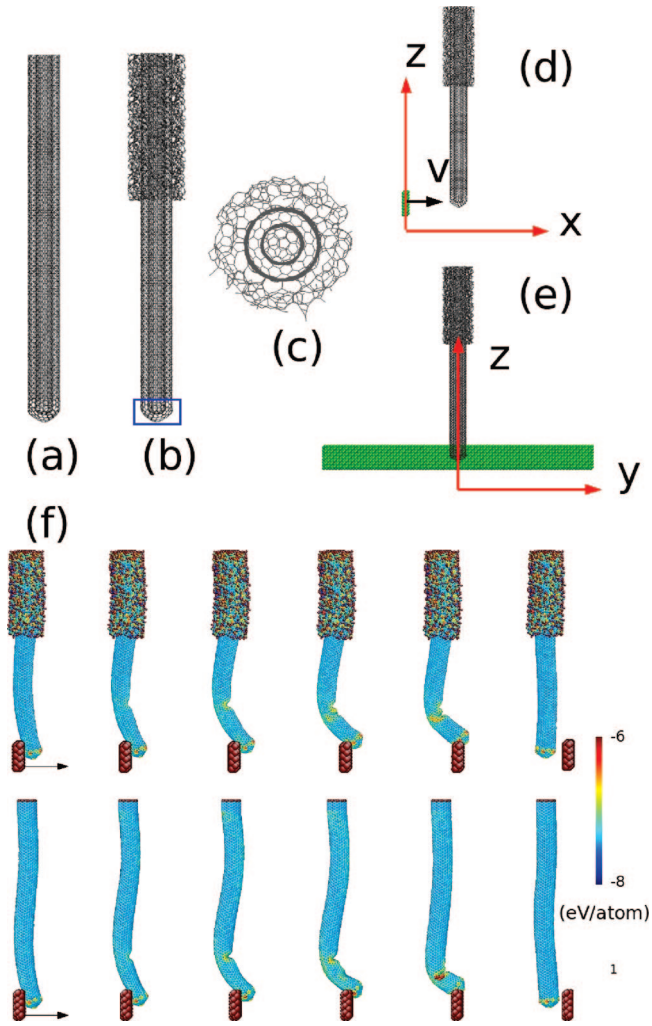

Figure 3. Lateral view of a double-walled carbon nanotube: (a) and with (b) a diamond-like shell (see text for details). The CNT extremity inside the rectangular region in (b) was used to follow the tip movement. (c) Top view of the CNT shown in (b). Lateral (d) and front (e) views of the CNT and the rigid obstacle that travels along the *X* direction. (f) Sequences of snapshots during the contact between tip models and the obstacle. Atoms are colored according to their potential energy.

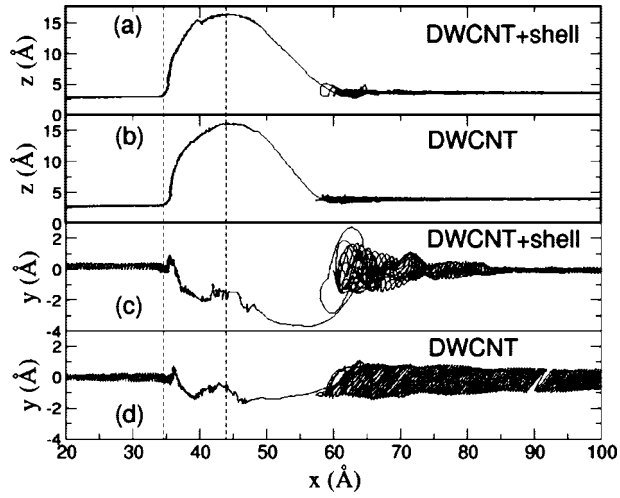

Figure 4. Tip extremity trajectory along $Z-X$ plane (a,b) and, $Y-X$ plane (c,d) during molecular dynamics simulations. The interaction between the tip and the obstacle occurs in the region between the dashed lines. Note the quick damping of oscillation along *Y* direction for the composite (DWCNT + shell) tip.

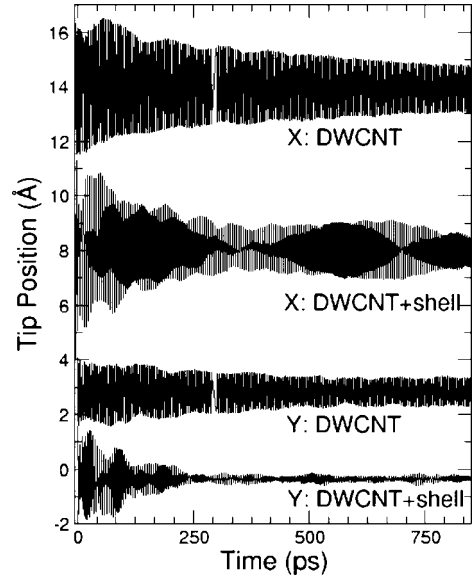

Figure 5. Movement of the tip extremity after losing contact with the obstacle. The curves were shifted upward to help visualization. Note the quick damping of oscillation along *Y* direction for the composite tip.

aspects of the reinforcement of CNT nanocomposite tips, computer simulations were performed.

We have investigated the effect of a diamond-like layer covering some length of a CNT using molecular dynamics simulations based on adaptive intermolecular reactive empirical bond-order potential.[27] This potential is similar to the reactive potential developed by Brenner,[28] but it incorporates the nonbonded interactions by suitable modifications through an adaptive treatment of the intermolecular interactions. This kind of reactive potentials have been proved to be accurate to describe carbon nanotube deformation under mechanical loads.[29,30]

Because simulations involving the multishell CNTs used in experiments (10–30 nm in diameter) are computationally prohibitive, we have analyzed two probe tip models of smaller size: (a) a double wall CNT (DWCNT, diameter 1.49 nm) tip 17.7 nm in length (Figure 3a) and (b) a composite tip formed by the same CNT but covered partially with a diamond-like carbon shell 0.7 nm in thickness and 7.2 nm long (Figure 3b). For the composite tip, we have induced the formation of chemical bonds between CNT and the covering shell by initially setting the atomic position at a very close distance from a perfectly formed graphitic CNT (Figure 3c). Atoms in the top extremity of the tip (1 nm in length) were kept fixed during the simulations, mimicking the attachment of the CNT to a rigid surface. The Berendsen's thermostat[31] was applied in atoms within a region of 3.5 nm in length from the top to mimic the transfer of thermal energy from the CNT to the rigid surface to which it is attached and to keep the temperature at 300 K. The remaining atoms were allowed to evolve in time according to Newton's equations of motion without constraints. The equations of

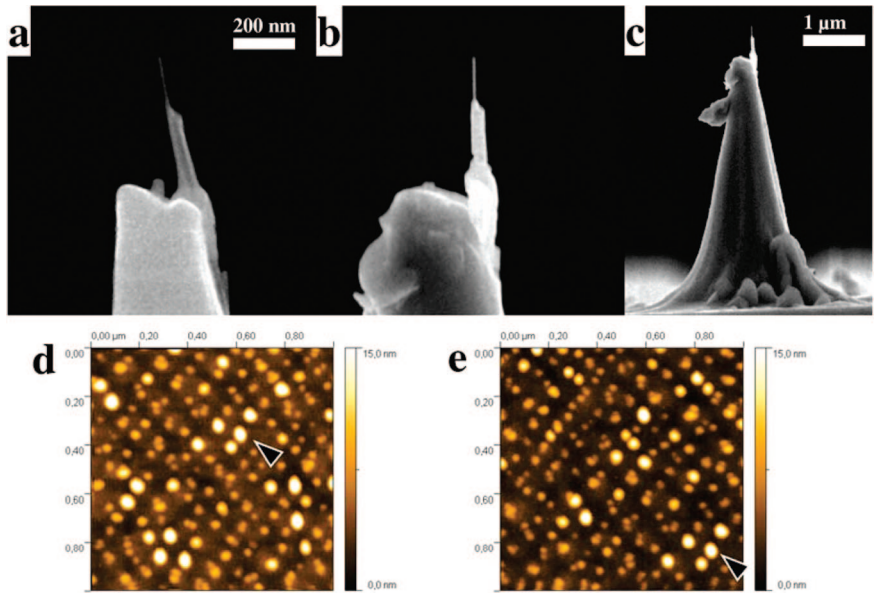

Figure 6. Application of a high aspect-ratio AFM tip based on a CNT composite. (a) Close view of the composite tip ready for AFM imaging. (b) Detailed view of the same tip (but from another angle) after taking 400 AFM images; note that no degradation can be detected. (c) Low magnification image of the AFM tip in (b). (d,e) Atomic force microscopy images of InAs quantum dots (average dot size is 26 ± 6 nm in diameter and 6 ± 1 nm in height) grown on InP substrate[37] acquired in tapping mode (1 μm × 1 μm scan area). (d) Typical image acquired just after first use of the composite tip. (e) Image of the same sample region after acquiring 400 scanning (an arrow helps to identify identical dots). Since many hours have passed between the acquisition of the two AFM images, a non-negligible drift is observed for these images. The image lateral resolution is equivalent to that usually obtained with high resolution commercial Si tips. No degradation of image lateral or vertical resolution was detected (see Supporting Information Figure S2).

motion were integrated with a third-order Nordisieck predictor-corrector algorithm[32] using a time step of 0.5 fs. The tips described above were dragged along a rigid obstacle (1.2 nm higher than the CNT extremity, Figure 3d,e) with a constant velocity of 10 m/s along the *X* axis.

To visualize the CNT deformation, Figure 3f shows snapshots of the simulations during the contact with the obstacle. Both tips return to their original form after the contact with no plastic deformation, but the tips displayed a quite different deformation pattern for the DWCNT with and without the diamond-like shell (see videos 1 and 2 included in Supporting Information). For example, the composite region shows negligible distortion and the deformation is mostly absorbed by the protruding CNT region, which is in accordance with the experimental observation (Figure 2).

A more detailed insight can be obtained by analyzing the trajectories of the tip extremity (indicated with a rectangle in Figure 3b) during the simulations. Considering the displacement in the vertical $X-Z$ plane, similar behaviors are observed (Figure 4a,b). On the other hand, the movement in the $X-Y$ plane is very different; the composite tip displays a larger lateral displacement than that of the pure CNT case (compare Figure 4c,d). This can be accounted for by the fact that the total vertical tip displacement to pass over the obstacle must be absorbed by laterally deforming the much shorter (also stiffer) CNT region protruding from the diamond-like shell, which is rendered easier by allowing a larger bending perpendicular (along *Y* axis) to the obstacle.

At this point, it is important to analyze the tip motion after loosing contact with obstacle when it starts an oscillatory movement. As mentioned above, initially, the composite tip displays larger amplitude than the simple CNT (Figure 5), but subsequently the amplitude damping is much faster for the nanotube with the diamond-like shell. The composite tip faster amplitude decay (strong damping) is clearly visible for the *Y* direction, while the pure CNT oscillations display much slower amplitude reduction. In addition, looking at the frequency of the tip oscillations, it is clear that the addition of the diamond-like shell has significantly raised it; this can be easily noted by looking at the reduction of vibration period along *X* axis in Figure 5. The frequency rise is associated with the increase of system stiffness associated with the shortening of the uncovered CNT region. As the composite tip response can be described by the coupling of two bending beams (the covered and free CNT regions), a beating phenomena may arise;[33] this phenomenon is clearly visible as a long period (low frequency) envelope around the *X* axis displacement. Briefly, the simulation results point out that the presence of a diamond-like shell not only increases the oscillation frequency but also serves as a vibration damper, in excellent agreement with experimental observations.

Finally, to evaluate wear and strength in a practical nanoscience application, we have used a composite C-CNT tip as an AFM probe (see Figure 6a).[34] The sample chosen for this study contains laterally ordered self-assembled InAs quantum dots grown on a GaAs substrate by chemical beam epitaxy.[35] AFM images were obtained in-air by noncontact mode (MI PicoPlus and AutoProbe CP from ThermoMicroscopes). For the sake of comparison, the sample was also imaged using standard conical Si tips (model UL-06, tip radius 10 nm, angle 12°). Using the composite probes, images were generated with excellent vertical and lateral resolution;[36] moreover, no reduction of imaging capabilities was observed after taking 400 images (compare images in Figure 6d,e, see

also image profiles in Supporting Information Figure S2). Although commercial high resolution Si tips yield images of equivalent quality, image resolution degrades after mere 10–20 images. A close analysis of the tip structure and morphology after acquisition of 400 images shows no signs of degradation (Figure 6b,c). In addition, the resilient properties of our composite probe also contribute to its extended lifetime when compared to Si tips because a common cause for tip wear and loss of lateral resolution is the damage inflicted to the tip apex during sample approach.

In summary, we have shown that high aspect ratio nanotools can be easily generated by associating the extreme mechanical properties of CNTs with hard amorphous carbon; unsuitable properties such as flexibility and vibration can be controlled without deteriorating the excellent CNT attributes: size, aspect ratio, strength, and resilience. The behavior of this system was experimentally and theoretically studied. Finally, these composite tips showed excellent wear resistance and high resolution imaging capabilities when used as AFM probes. No degradation of tip or image quality was detected after taking 400 images. Further work is in progress to improve the nanocomposite tip mechanical properties by a careful control of the amorphous carbon layer and also test the composite tips as tools for nanomanipulation.

Acknowledgment. This work was supported by LNLS, FAPESP, and CNPq. We thank P.C. Silva (LME-LNLS) for assistance during nanomanipulation experiments.

Supporting Information Available: Amorphous carbon tip generated by EBD on a W wire. Time evolution of the motion of the composite tip model. Time evolution of the motion of the double-wall CNT tip model. This material is available free of charge via the Internet at http://pubs.acs.org.

References

(1) Yu, M. F.; Lourie, O.; Dyer, M. J.; Moloni, K.; Kelly, T. F.; Ruoff, R. S. *Science* **2000**, *287*, 637.
(2) Kim, K. S.; Lim, S. C.; Lee, I. B.; Na, K. H.; Bae, D. J.; Choi, S; Yoo, J.-E.; Lee, Y. H. *Rev. Sci. Instrum.* **2003**, *74*, 4021.
(3) St. Fahlbusch, S.; Mazerolle, J.- M.; Breguet, A.; Steinecker, J.; Agnus, R.; Pérez, J.; Michler, *J. Mater. Process. Tech.* **2005**, *167*, 371.
(4) Nakabayashi, D.; Silva, P. C.; González, J. C.; Rodrigues, V.; Ugarte, D. *Microsc. Microanal.* **2006**, *12*, 311.
(5) Matsuda, I.; Ueno, M.; Hirahara, T.; Hobara, H.; Morikawa, H.; Liu, C.; Hasegawa, S. *Phys. Rev. Lett.* **2004**, *93*, 236801.
(6) Guise, O.; Marbach, H.; Yates, J. T., Jr.; Jung, M.-C.; Levy, J.; Levy, J. *Rev. Sci. Instrum.* **2005**, *76*, 045107.
(7) Lin, X.; He, X. B.; Yang, T. Z.; Guo, W.; Shi, D. X.; Gao, H.-J.; Ma, D. D. D.; Lee, S. T.; Liu, F.; Xie, X. C. *Appl. Phys. Lett.* **2006**, *89*, 043103.
(8) Walton, A. S.; Allen, C. S.; Critchley, K.; Górzny, M L.; McKendry, J. E.; Brydson, R. M. D.; Hickey, B. J.; Evans, S. D. *Nanotechnology* **2007**, *18*, 065204.
(9) Junno, T.; Carlsson, S.-B.; Hongqi, X.; Montelius, L.; Samuelson, L. *Appl. Phys. Lett.* **1998**, *72*, 548.
(10) Falvo, M. R.; Clary, G. J.; Taylor, R. M., II; Chi, V.; Brooks, F. P., Jr.; Washburn, S.; Superfine, R. *Nature* **1997**, *389*, 5827.
(11) Nakabayashi, D.; Silva, P. C.; Ugarte, D. *Appl. Surf. Sci.* **2007**, *254*, 405.
(12) Iijima, S. *Nature* **1991**, *354*, 56.
(13) Konishi, H.; Murata, Y.; Wongwiriyapan, W.; Kishida, M.; Tomita, K.; Motoyoshi, K.; Honda, S.; Yoshimoto, S.; Kubo, K.; Hobara, R.; Matsuda, I.; Hasegawa, S.; Yoshimura, M.; Lee, J.-G.; Mori, H.; Katayama, M. *Rev. Sci. Instrum.* **2007**, *78*, 013703.
(14) Yoshimoto, S.; Murata, Y.; Kubo, K.; Tomita, K.; Motoyoshi, K.; Kimura, T.; Okino, H.; Hobara, R.; Matsuda, I.; Honda, S.; Katayama, M.; Hasegawa, S. *Nano Lett.* **2007**, *7*, 956.
(15) Nakabayashi, D.; Silva, P. C.; Ugarte, D. *Int. J. Nanotechnol.* **2007**, *4*, 609.
(16) Poncharal, P.; Wang, Z. L.; Ugarte, D.; de Heer, W. A. *Science* **1999**, *283*, 1513.
(17) Treacy, M. M.; Ebbesen, T. W.; Gibson, J. M. *Nature* **1996**, *38*, 678.
(18) www.nano.gov/NNI_Instrumentation_Metrology_rpt.pdf
(19) Callister, W. D., Jr.; *Materials Science and Engineering: An Introduction*, 6th ed.; John Wiley & Sons: Hoboken NJ, 2003.
(20) Akama, Y.; Nishimura, E.; Sakai, A.; Murakami, H. *J. Vac. Sci. Technol., A* **1990**, *8*, 429.
(21) Wendel, M.; Lorenz, H.; Kotthauss, J. P. *Appl. Phys. Lett.* **1995**, *67*, 3732.
(22) Chen, X; Zhang, S.; Dikin, D. A.; Ding, W.; Ruoff, R. S. *Nano Lett.* **2003**, *3*, 1299.
(23) Ding, W.; Dikin, D. A.; Chen, X.; Piner, R. D.; Ruoff, R. S.; Zussman, E.; Wang, X.; Li, X. *J. Appl. Phys.* **2005**, *98*, 014905.
(24) Chen, X. Q.; Zhang, S. L.; Dikin, D. A.; Ding, W. Q.; Ruoff, R. S.; Pan, L. J.; Nakayama, Y. *Nano Lett.* **2003**, *3*, 1299–1304.
(25) Hoffmann, S.; Utke, I.; Moser, B.; Michler, J.; Christiansen, S. H.; Schmidt, V.; Senz, S.; Werner, P.; Gösele, U.; Ballif, C *Nano Lett.* **2006**, *6*, 622.
(26) Rong, W.; Ding, W.; Ma1dler, L.; Ruoff, R. S.; Friedlander, S. K. *Nano Lett.* **2006**, *6*, 2646.
(27) Stuart, S. J.; Tutein, A. B.; Harrison, J. A. *J. Chem. Phys.* **2000**, *112*, 6472.
(28) Brenner, D. W. *Phys. Rev. B* **1990**, *42*, 9458.
(29) Yakobson, B. I.; Brabec, C. J.; Bernholc, J. *Phys. Rev. Lett.* **1996**, *76*, 2511.
(30) Garg, A.; Han, J.; Sinnott, S. B. *Phys. Rev. Lett.* **1998**, *81*, 2260.
(31) Berendsen, H. J. C. *J. Chem. Phys.* **1984**, *81*, 3684.
(32) Allen, M. P.; Tildesley, D. J. *Computer Simulation of Liquids*; Oxford University Press: New York, 1987.
(33) Inman, D. J. *Engineering Vibration*: Prentice Hall: Upper Saddle River, NJ, 2000.
(34) Dai, H. J.; Hafner, J. H.; Rinzler, A. G.; Colbert, D. T.; Smalley, R. E. *Nature* **1996**, *384*, 147.
(35) Bortoleto, J. R. R.; Gutiérrez, H. R.; Bettini, J.; Cotta, M. A. *Appl. Phys. Lett.* **2005**, *87*, 013105.
(36) Gutiérrez, H. R.; Nakabayashi, D.; Silva, P. C.; Bortoleto, J. R. R.; Rodrigues, V.; Clerici, J. H.; Cotta, M. A.; Ugarte, D. *Phys. Status Solidi A* **2004**, *201*, 888.
(37) Bortoleto, J. R. R.; Zelcovit, J. G.; Gutiérrez, H. R.; Bettini, J.; Cotta, M. A. *Nanotechnology* **2008**, *19*, 015601.

NL0729633